Thin Solid Films 615 (2016) 366–373

Contents lists available at ScienceDirect

Thin Solid Films

journal homepage: www.elsevier.com/locate/tsf

Agitation dependent properties of copper indium diselenide thin films prepared by electrochemical route

Ashwini B. Rohom, Priyanka U. Londhe, Nandu B. Chaure *

Electrochemical laboratory, Department of Physics, Savitribai Phule Pune University, Pune, 411007, India

ARTICLE INFO

Article history:
Received 9 December 2015
Received in revised form 21 July 2016
Accepted 21 July 2016
Available online 25 July 2016

Keywords:
$CuInSe_2$
Agitation
Electrodeposition
Cyclic voltammetry
X-ray diffraction
Stoichiometric layer

ABSTRACT

$CuInSe_2$ (CIS) thin films have been prepared by potentiostatic electrochemical synthesis route in an aqueous medium. A conventional three-electrode electrochemical geometry was used to study the influence of agitation on electrodeposition of CIS. The co-deposition potentials for Cu-In-Se, −0.4 V and −0.6 V were optimized by using cyclic voltammetry measurements. The diffusive controlled growth with instantaneous nucleation is observed by Chronoamperometric measurements. X-ray diffraction (XRD) and Raman spectroscopy, UV–Vis spectroscopy, energy dispersive X-ray analysis (EDAX) and scanning electron microscopy (SEM) were employed to study the structural, optical, compositional and morphological properties, respectively. Polycrystalline CIS thin films with tetragonal structure were obtained without agitation, however the secondary phases of Cu_xSe_y were attributed with agitation. The Raman results are found to be in good agreement with XRD and EDAX analyses. Without agitation the energy band gap (Eg) was estimated ~1.1 eV. The higher values of Eg ~ 1.5 to 1.8 eV measured for the samples grown with agitation are proposed due to the inhomogeneous growth of precursors and the change in surface morphology. Uniform, compact and well adherent CIS layers were deposited with and without agitation. The deposition potentials and agitation conditions were found to be greatly affected on the surface morphology. The stoichiometric CIS layer was deposited at −0.6 V without agitation.

1. Introduction

Thin film solar cells such as, $CuInSe_2$ (CIS), $CuInGaSe_2$ (CIGS) and cadmium telluride (CdTe) are an excellent candidate for clean energy generation with significantly lower production cost. CIS is I-III-VI group semiconductor having direct band-gap (1.04 eV) and high absorption coefficient (10^4 cm^{-1}). The highest efficiency for CIGS based solar cells devices is ~21.7%, reported by ZSW group, Germany [1,2]. Numerous reports are available on fabrication of CIS solar cells by vacuum and non-vacuum techniques such as co-evaporation [3], sputtering [5], spray pyrolysis [6], molecular beam epitaxy [7], stacking elemental layers [8], flash evaporation [9], pulsed laser deposition [10] and electrodeposition [11], etc. Electrodeposition is a versatile method for the preparation of thin films of metals, insulator and semiconductors, because of its simplicity and high throughput [13,14]. Since decades the electrodeposition has been widely employed for the preparation of solar cell devices. CIGS and CdTe are the leading photovoltaic materials, which have been successfully deposited using electrodeposition at an industrial level [14–16]. Bhattacharya et al., [17] reported the highest efficiency 15.4% for CIGS solar cells prepared by electrodeposition technique. Numerous reports are available on the electrodeposition of CIS layers by one-step electrodeposition, selenization of electrodeposited Cu-In alloy thin films and pulsed electrodeposition [18–20]. Agitation is one of the important parameters during the electrochemical synthesis to control the deposition rate, stoichiometry, mass transport, surface morphology, etc. Nakamura et.al, [21] deposited CIS thin films with and without agitation and studied the dependence of composition or ratio of mass transfer coefficient. Agitation in the plating electrolyte can be produced either by stirring an electrolyte or rotating the working electrode, which is commonly known as rotating disc electrode. Herein we have reported the deposition of stoichiometric CIS thin films by electrodeposition technique without agitation on fluorine doped tin oxide (FTO) coated glass substrates. Herein, we examined the effects of electrolyte agitation during deposition process by comparing them with deposited sample without electrolyte agitation. Furthermore, the influence of agitation on the morphological, structural and chemical compositions of deposited CIS material was also thoroughly investigated.

2. Experimental details

Ppotentiostatic electrodeposition with a standard three-electrode geometry was used for the deposition of CIS thin films. FTO coated glass substrate, Ag/AgCl and graphite were used as working, reference and counter electrodes, respectively. The electrolyte was prepared in aqueous medium consisting of 3 mM copper chloride ($CuCl_2$), 6 mM indium chloride ($InCl_3$) and 3 mM selenous acid (H_2SeO_3). Lithium chloride was used as a supporting additive. The pH of the bath was adjusted to 1.2 with dilute HCl. The deposition parameters were optimized by studying the cyclic voltammetry for different agitation speeds,

http://dx.doi.org/10.1016/j.tsf.2016.07.052
0040-6090/

viz. 0 rpm, 100 rpm and 200 rpm. Above 200 rpm the samples were not adherent to the substrate. CIS layers were electrodeposited at −0.4 V and −0.6 V versus Ag/AgCl reference electrode. The films were dried in normal laboratory ambient and used for further characterizations.

A μ3AUT 70762 AUTOLAB potentiostat/galvanostat was used for cyclic voltammetry studies and electrodeposition of the CIS layers. The structural properties were studied by means of X-ray diffraction (XRD), model Bruker D8 advance diffractometer with Cu Kα anode of wavelength 0.154 nm and Invia Renishow micro Raman spectrophotometer, with 785 nm excitation laser. Optical absorption measurements were carried out by JASCO UV–Vis-NIR spectrophotometer. JEOL JSM 6360 A, scanning electron microscope with an accelerating voltage 20 kV was used to study the surface morphology. The elemental atomic percentage concentrations were obtained by energy dispersive X-ray analysis technique equipped with the SEM unit.

3. Results and discussion

The cyclic voltammetry measurements were performed to optimize the co-deposition potential of Cu-In-Se in presence of LiCl at room temperature. The cyclic voltammograms obtained without agitation and for 100 and 200 rpm with scan rate 5 mV/s are depicted in Fig. 1 a), b) and c), respectively.

Initially, at lower cathodic potentials up to −0.4 V, the features noticed are associated to the reduction of Cu and Se by the following charge-transfer reactions,

$$Cu^{2+} + 2e^- \rightarrow Cu \qquad E_0 = +0.34 \text{ V versus SHE} \quad (1)$$

$$H_2SeO_3 + 4e^- + 4H^+ \rightarrow Se + 3H_2O \qquad E_0 = +0.74 \text{ V versus SHE} \quad (2)$$

Indium is proposed to be electrodeposited along with Cu and Se to deposit ternary alloy of CIS in the plateau region observed about −0.4 V to −0.7 V by the charge transfer reaction,

$$In^{3+} + 3e^- \rightarrow In \qquad E_0 = +0.74 \text{ V versus SHE} \quad (3)$$

CIS layers can be electrodeposited by the following charge reaction,

$$Cu^{2+} + In^{3+} + 2SeO_3{}^{2-} + 9e^- + 12H^+ \rightarrow CuInSe_2 + 6H_2O \quad (4)$$

The current enhancement observed without agitation (Fig. 1(a)) at lower cathodic potentials (+0.1 V to −0.4 V) marked as 'A' is proposed due to the reduction of Cu and Se ions. This region may favor the deposition of secondary phases of Cu_xSe_y [18]. A flat limiting current plateau, which is nearly unaffected by the growth potential observed in the

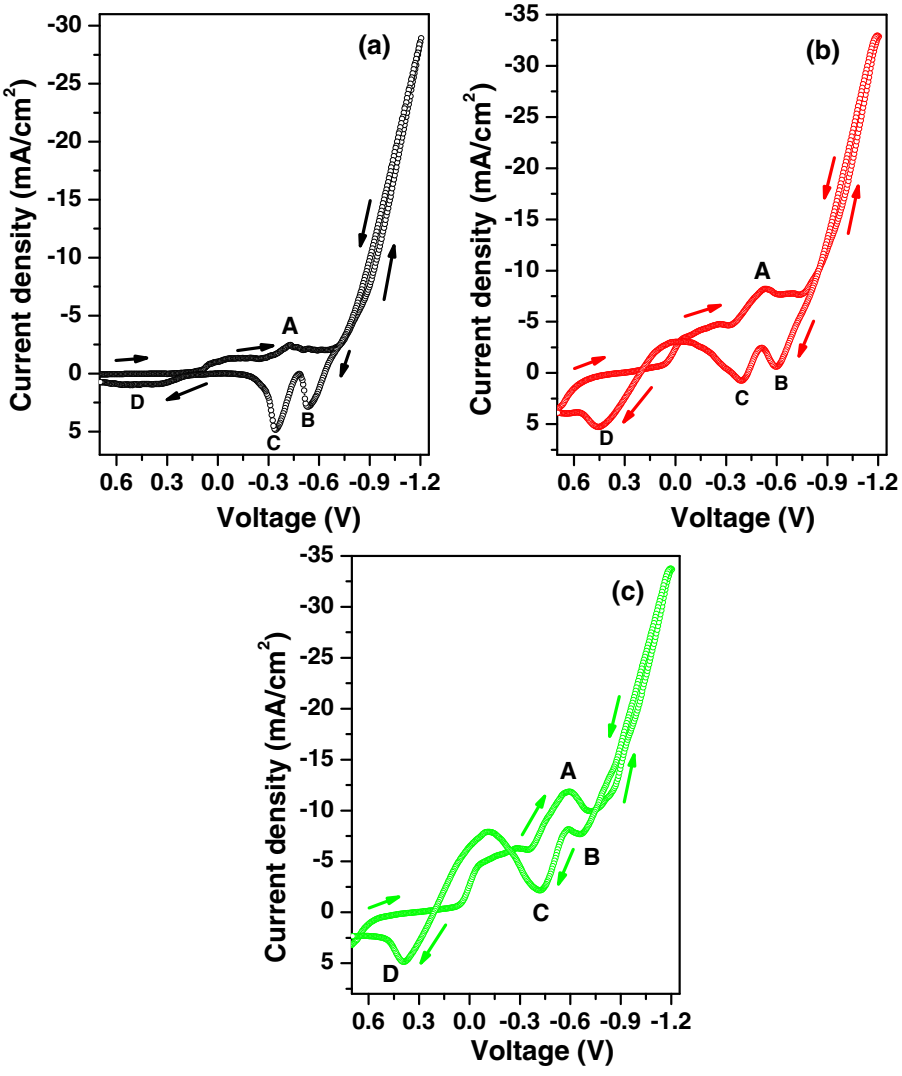

Fig. 1. Cyclic voltammograms recorded in the matrix of Cu, In and Se precursors in an aqueous bath at room temperature for different agitation speeds a) 0 rpm, b) 100 rpm and c) 200 rpm with scan rate of 5 mV s^{-1}.

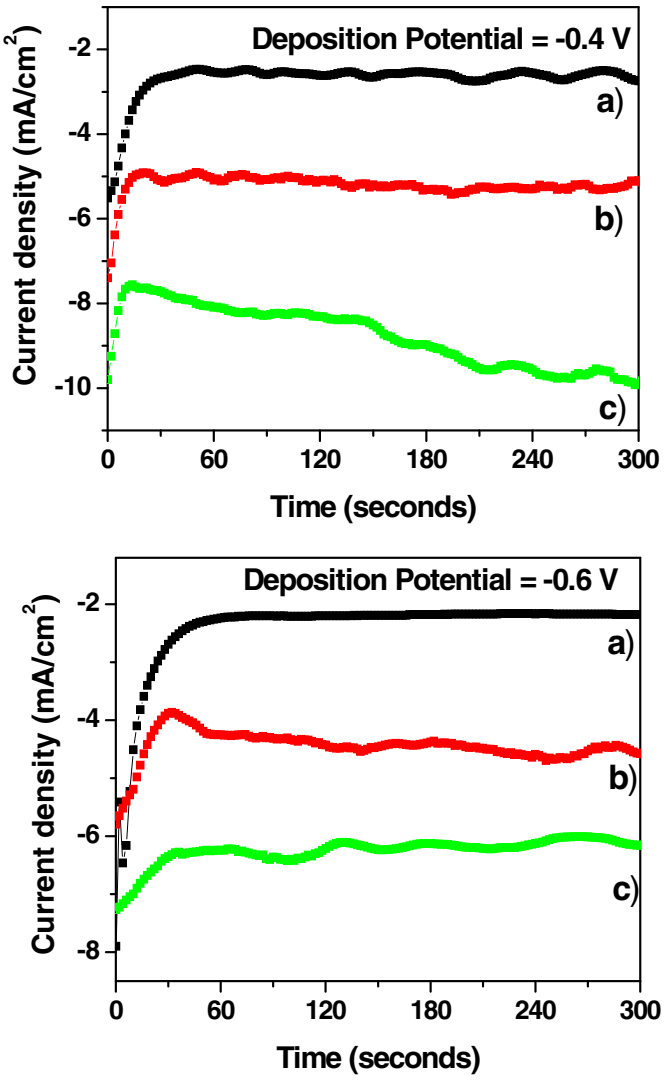

Fig. 2. Chronoamperometric curves on potentiostatic deposition of CIS under different agitation speeds 0 rpm, b) 100 rpm and c) 200 rpm at different deposition potentials.

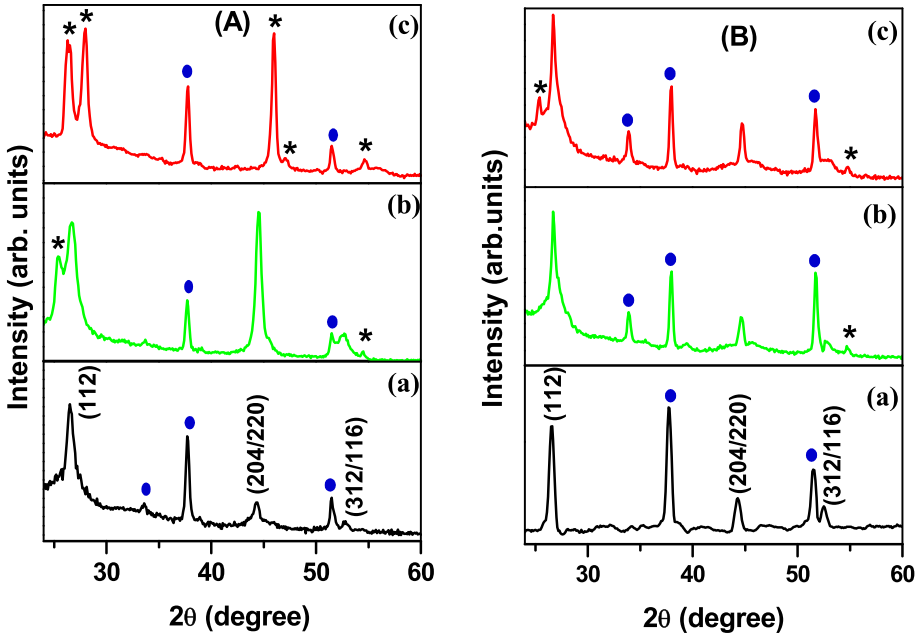

Fig. 3. XRD patterns of CIS thin films deposited at −0.4 V A) and −0.6 V B) for agitation speeds a) 0 rpm, b) 100 rpm and c) 200 rpm on FTO coated glass substrates. (●) and (*) represent the peak associated to FTO and CuSe.

Table 1
A summary of the XRD results for obtained the CIS layers deposited at −0.4 V and −0.6 V with different agitation speeds.

Agitation speed	2θ (deg)				'd' (A^0)				Miller indices *(hkl)*		Structural assignment	
	Observed		Standard		Observed		Standard					
Deposition potential (V)	−0.4	−0.6	−0.4	−0.6	−0.4	−0.6	−0.4	−0.6	−0.4	−0.6	−0.4	−0.6
	26.52	26.63	26.62	26.62	3.357	3.345	3.352	3.345	(112)	(112)	CIS	CIS
0 rpm	44.32	44.41	44.28	44.28	2.041	2.043	2.043	2.043	(204/220)	(204/220)	CIS	CIS
	52.49	52.56	52.41	52.41	1.741	1.744	1.744	1.744	(116/312)	(116/312)	CIS	CIS
	25.82	26.61	26.42	26.62	3.446	3.370	3.345	3.345	(111)	(112)	CuSe	CIS
	26.63	44.55	26.62	44.28	3.343	3.345	2.031	2.043	(112)	(204/220)	CIS	CIS
100 rpm	44.41	52.66	44.28	52.41	2.037	2.043	1.736	1.744	(204/220)	(116/312)	CIS	CIS
	52.56	54.61	52.41	54.39	1.739	1.744	1.678	1.685	(116/312)	(222)	CIS	CuSe
	54.51		54.39		1.681		1.685		(222)		CuSe	
	25.88	25.52	26.42	26.42	3.438	3.486	3.370	3.370	(111)	(111)	CuSe	CuSe
	28.01	26.61	27.92	26.62	3.181	3.345	3.192	3.345	(112)	(112)	CuSe	CIS
200 rpm	45.93	44.61	45.28	44.28	1.973	2.028	2.001	2.043	(117)	(204/220)	CuSe	CIS
	46.16	52.86	45.89	52.41	1.964	1.729	1.976	1.744	(200)	(116/312)	CuSe	CIS
	54.61	54.71	54.39	54.39	1.678	1.675	1.685	1.685	(222)	(222)	CuSe	CuSe

range −0.42 V to −0.62 V is assigned the diffusion controlled electrodeposition. The increase in cathodic current density with increasing the agitation speed can be justified by the enhanced diffusion of Cu^{2+} to the electrode, yielding higher amount of Cu^{2+} near the cathode during the initial process of reduction [22]. The shift in peak appeared due to charge transfer reaction of Cu and Se towards more cathodic potential is observed after agitation, also electrolyte agitation induces a progressive shift of both cathodic as well as anodic peaks to more negative and positive values, respectively. Polycrystalline and controlled stoichiometric CIS layers may be obtained in this plateau region. The sharp rise in the cathodic current observed beyond −0.65 V is proposed due the hydrogen evolution as well as the metallic deposition of In. A plateau region is found to be shifted towards the higher cathodic potential with increase in the agitation speed due to the change in open circuit potentials (OCP) and/or pH in the vicinity of working electrode. The values of OCP, +0.33, +0.39 and +0.43 V, were measured for the CIS layer deposited for different agitation rate from 0 rpm, 100 rpm and 200 rpm, respectively. Furthermore, a cathodic current density was also found to be increased with increase in the agitation speed of the solution. The anodic or stripping peaks are associated with the redox potentials of precursors. Moreover, the element having more negative redox potential is expected to deposit at the end or high cathodic potentials. According to the half electrode reactions e1, 2 and 3 given in the manuscript, one can assign the peaks B, C and D could be corresponds the stripping of In, Cu and Se.

Fig. 2 shows the Chronoamperometric curves of CIS for deposition potentials −0.4 V and −0.6 V with and without agitation of electrolyte. It is observed that the current density increases with increase in agitation rate. At the beginning of the curves, the cathodic current was sharply decreases within first few seconds in all cases and later nearly remains constant. This type of behavior is associated with the diffusive controlled growth with instantaneous nucleation, while the rapid drop in current density at the initial stage is due to the double layer charging/discharging [23]. According to the electrochemical point of view, the deposition can occur due to mass transport, diffusion, migration and convection [24]. The migration is the delivery of metal ions, therefore, the main driving forces contributing to electrodeposition are derived from a concentration gradient (diffusion) and movement of the reacting species (convection) [25]. The movement of the bulk solution by electrolyte agitation generally results in an enhancement of the convection, giving rise to the vigorous delivery of metal ions to the cathode surface. The Chronoamperometric curves confirm the instantaneous nucleation and the process is diffusion limited, therefore, the diffusion

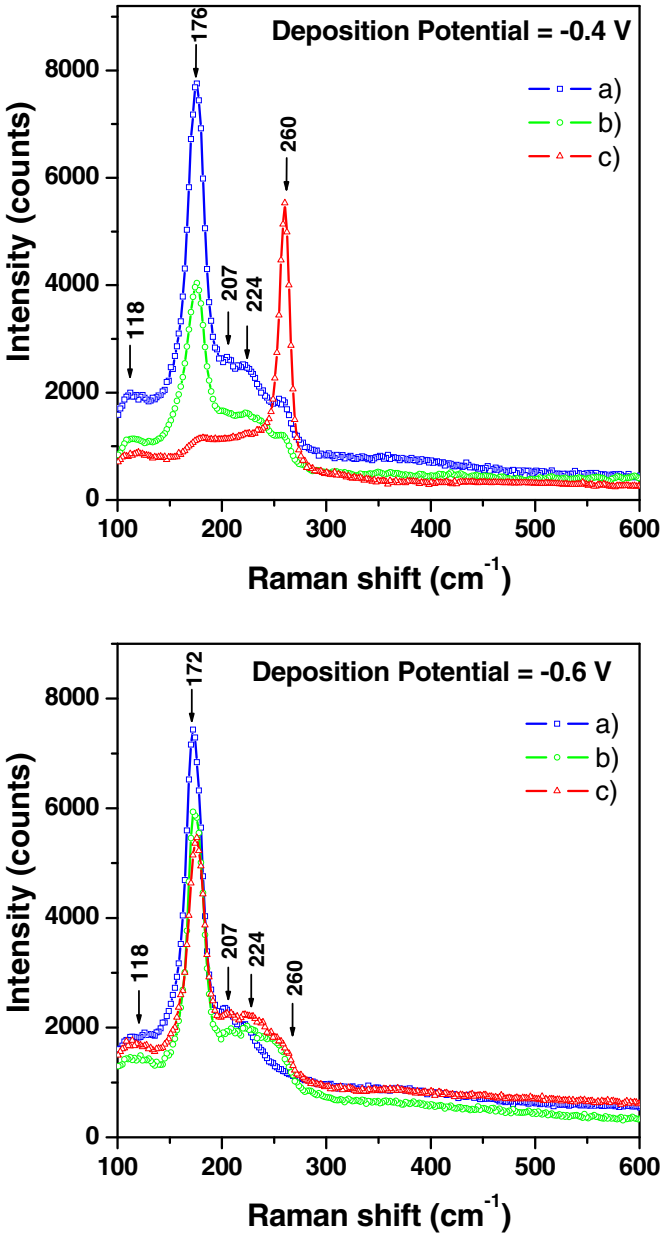

Fig. 4. Raman spectra for CIS thin films deposited at −0.4 V and −0.6 V under various electrolyte agitation speeds a) 0 rpm, b) 100 rpm and c) 200 rpm.

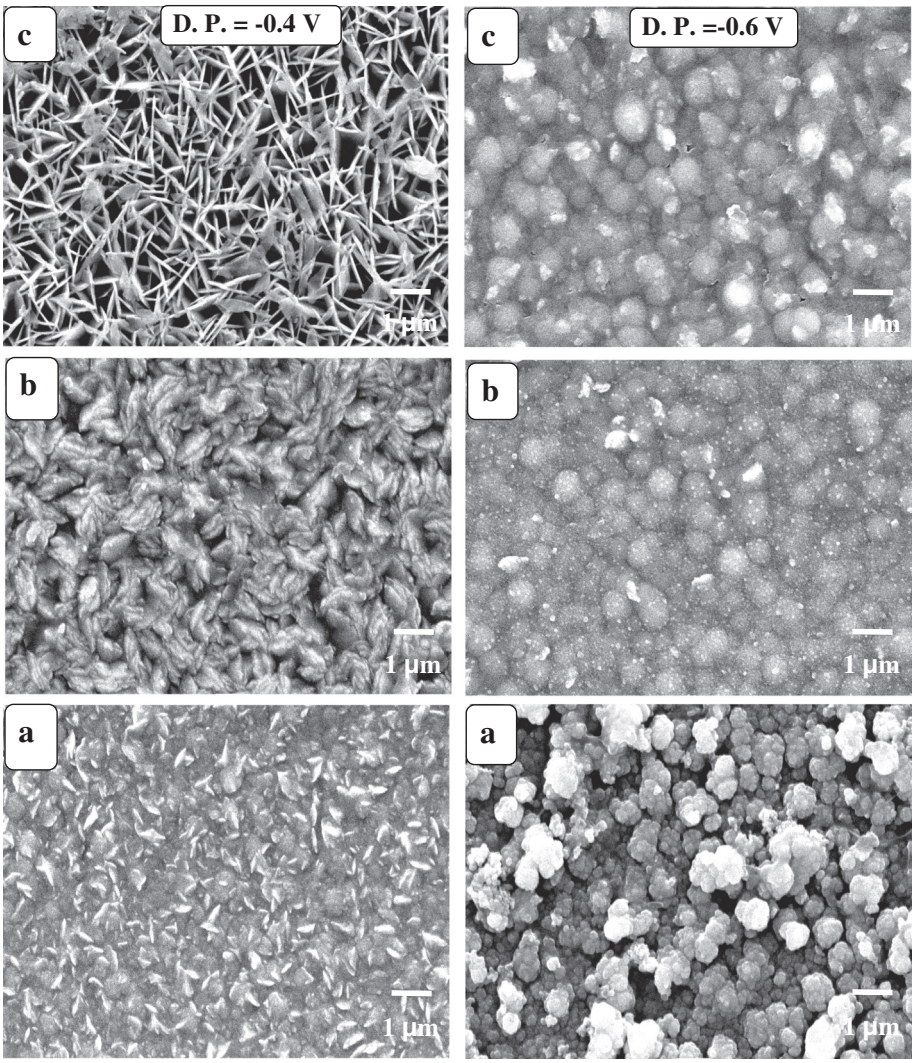

Fig. 5. SEM Images of CIS thin films deposited at −0.4 V and −0.6 V for different agitation speeds a) 0 rpm, b) 100 rpm and c) 200 rpm.

layer can be related to limiting current density (i_L) expressed as [26]

$$i_L = zFD\frac{C}{\delta_N}$$

where, z is the number of electrons of a metal ion, F is Faraday's constant, D is the diffusion coefficient, C is the ion concentration of bulk solution and δ_N is the diffusion-layer thickness. Since the terms z, F and D are constant, and ionic concentrations was used with and without agitations were also constant. Thus, the diffusion-layer thickness is the only factor depends on the limiting current density. As the stirring rate increases the limiting current density increases which thereafter decrease the diffusion layer thickness [27]. This information is used for further structural, morphological and chemical composition analysis.

Fig. 3 (A) shows the XRD pattern of CIS thin films deposited at −0.4 V for different agitation rates. The reflections (112), (204/220) and (312/116) corresponds to the tetragonal structure of CIS are attributed in the pristine CIS layer. It is noticed that without agitation the peaks associated to the CIS are exhibited with orientation along (112) plane. The layer deposited at 100 rpm exhibits the peak related to CIS along with binary phases of CuSe. The layer deposited at 200 rpm exhibit only the peaks related to CuSe. The XRD results agree well with elemental composition obtained by EDAX analysis, which is discussed in the next section. The peaks related to CuSe and FTO are marked as (⋆) and (●), respectively. Fig. 3 (B) shows the XRD pattern of CIS thin films deposited at −0.6 V for different agitation rates. Three prominent planes (112), (204/220) and (312/116) corresponds to tetragonal structure of CIS are attributed from the sample deposited without agitation, whereas the secondary peaks associated to CuSe are revealed in the sample deposited with agitation. The presence of secondary peaks associated to shift in deposition potential of CIS due to the change in open circuit potential with agitation. The XRD results are analyzed in detail and the observations are tabulated in Table 1.

The structural properties and the secondary phase formation in CIS layers was further studied using Raman spectroscopy with 785 nm excitation laser. Fig. 4 shows Raman spectra for CIS thin films grown at −0.4 V and −0.6 V under various agitation speeds. It is observed that CIS layers electrodeposited at −0.4 V with agitation at 0 rpm and 100 rpm shows the most intense peak at 176 cm^{-1}, which is associated to the vibrational A1 mode in the CIS chalcopyrite structure and the peaks attributed at 207 cm^{-1} and 224 cm^{-1} confirms the contribution of E and B2 modes of CIS phase [28]. The sharp peak exhibited at 260 cm^{-1} in the sample deposited at 200 rpm could be associated to the Cu-Se binary phase [29], which is not clearly observed in the sample deposited at 0 rpm and 100 rpm. The Raman results agree well with the XRD and EDAX analysis. Especially in the XRD analysis, the sample deposited at −0.4 V with 200 rpm the peaks associated to the formation of CIS were not observed, and the elemental concentrations determined by EDAX confirms the absence of In. Fig. 4 (B) shows the Raman spectra for CIS film grown at −0.6 V in presence of various agitation speeds. A

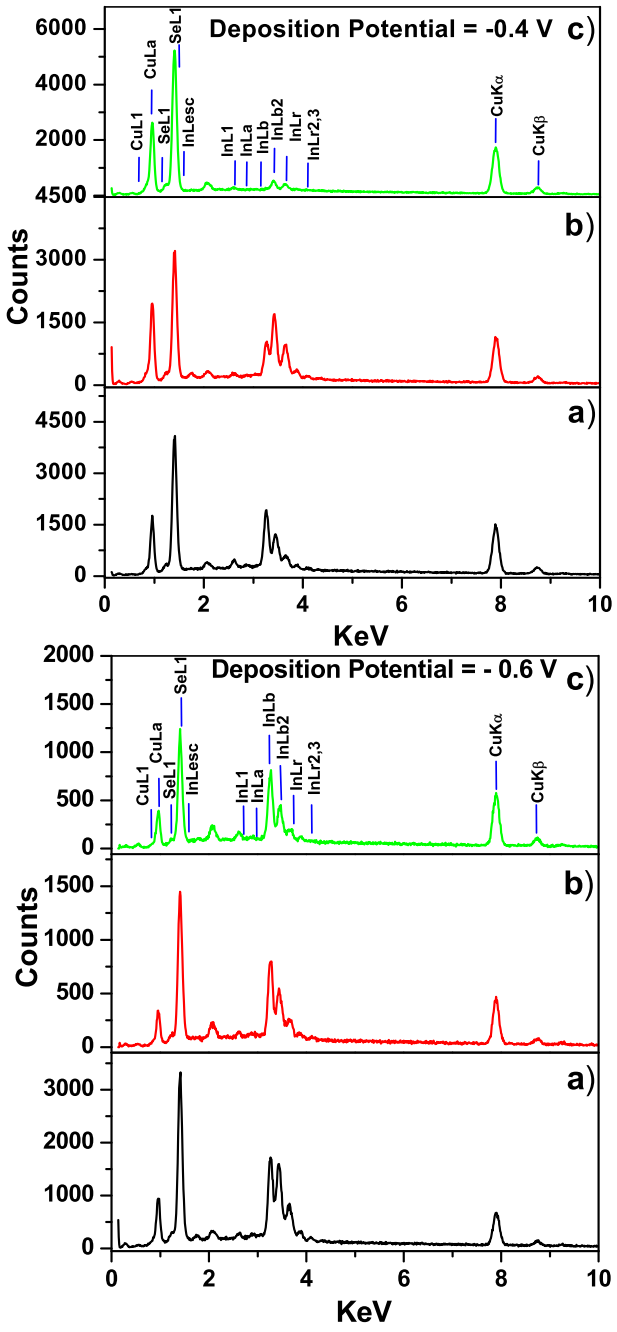

Fig. 6. EDAX of CIS thin films deposited at −0.4 V and −0.6 V on FTO coated glass substrates for different agitation speeds a) 0 rpm, b) 100 rpm and c) 200 rpm.

sample prepared without agitation showed only three peaks related to the chalcopyrite structure of CIS. The peaks associated to CIS are exhibited in all spectra, while a small hump observed around 260 cm^{-1} in agitated samples is related to secondary phase of the Cu-Se. A small shoulder appeared at 118 cm^{-1} is corresponds to the laser line used for the calibration of the Raman wave number.

The surface morphology was found to be dependent on the agitation and growth potentials. Layer deposited at −0.4 V and −0.6 V for without agitation were reasonably densely packed and compact. A remarkable change in the morphology consisting globular grains of size ~1 μm can be clearly seen for the layer deposited at −0.6 V without agitation. A randomly placed interdiffused disc shaped morphology was observed for the sample deposited at −0.4 V without agitation, which was found to be changed into agglomeration of particles upon agitation with 100 rpm. A seed like morphology covered all over the surface, densely packed, without void can be seen in Fig. 5 (b). For higher agitation speed (200 rpm) for the same growth potential (−0.4 V) the morphology was again changed to a randomly oriented flakes or longitudinal needles of size over a micron (Fig. 5 (c)). The voids are observed due to the random growth of the niddles. The diffused spherical grains of size over a micron are deposited at −0.6 V with agitation at 100 rpm and 200 rpm. The diffused grain with compact deposition is observed probably due to the elemental deposition of copper, which is further confirmed by EDAX analysis. The globular, compact and void free morphology observed for the sample electrodeposited at −0.6 V versus Ag/AgCl without agitation is desirable for the development of high efficiency CIS based thin film solar cell [13].

Fig. 6 (A) and (B) depicts the EDAX pattern of the layers electrodeposited at growth potentials −0.4 V and −0.6 V, respectively with and without agitation. The layers deposited at −0.4 V favors the deposition of Cu-rich material for both with and without agitation. The contents of Cu and In were found to be increased and decreased systematically with increasing the agitation speed during deposition. The increased Cu contents with increasing the agitation rate could be due to the diffusion limited reaction [19]. The contents of Se were also found to be increased upon the increasing the agitation speed. The layers deposited at 200 rpm were found only the contents of Cu and Se with nearly similar atomic percentages which are supported to the XRD results. The absence of In content could be related to the change in the open circuit potential measured with and without agitation. All the films deposited at −0.6 V with and without agitation was Cu-rich, moreover the contents of Cu further increased with agitation. The systematic change in the content of Cu and In was observed with increasing the agitation speed. As the layers were deposited at −0.4 V for three different agitation speeds 0 rpm, 100 rpm and 200 rpm, the actual potential applied between the electrode in presence of 200 rpm is less than that of the sample prepared without agitation (0 rpm) due to the change in the values of OCP from +0.33 to +0.43 V. At lower growth potentials only Cu and Se are expected to deposit. Therefore, due to the change in the OCP values the actual growth potential between with and without agitation is different. Thus the film grown at −0.4 V without stirring measured 15% In, while at 200 rpm In content was zero. To incorporate more In at 200 rpm, the cathodic growth potential need to be increased. Chassaing et al. have shown that In incorporation started beyond a potential value close to −0.6 V and In/Cu ratio increased towards more negative potential −0.6 V [30,31]. Some details are added in the revised manuscript and highlighted. The layers deposited without agitation at −0.6 V were found to be nearly stoichiometric close to the ideal concentration of CIS (Cu:In:Se = 25%:25%:50%). The variation in the contents of Cu, In and Se could be associated with the

Table 2
A summary of atomic concentration (%) of Cu, In and Se for CIS thin films deposited at −0.4 V and −0.6 V for different agitation speeds obtained by EDAX analysis.

Agitation speed	Deposition potential −0.4 V					Deposition potential −0.6 V				
	Atomic concentration (%)			In/Cu	Se/Cu	Atomic concentration (%)			In/Cu	Se/Cu
	Cu	In	Se			Cu	In	Se		
0 rpm	41.06	15.92	43.02	0.39	1.05	28.67	21.77	49.56	0.76	1.73
100 rpm	44.41	09.32	46.28	0.21	1.04	45.29	17.56	37.14	0.39	0.82
200 rpm	47.13	00.00	52.87	0.00	1.29	52.56	16.50	30.93	0.31	0.59

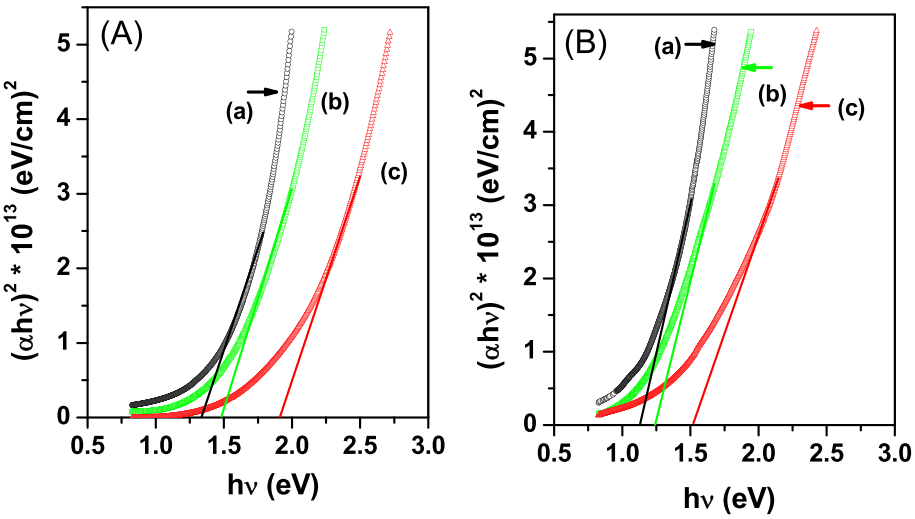

Fig. 7. UV–Vis absorption spectra of CIS thin films deposited at −0.4 V A) and −0.6 V B) for different agitation speeds a) 0 rpm, b) 100 rpm and c) 200 rpm.

formation of diffusion layer in the vicinity of working electrode. An enhancement in the limiting current density may also be related to the formation of highly conducting diffusion layer. The increase in limiting current density may leads to a metallic (copper) deposition at potential which is effectively lower than the specified one [32]. In/Cu and Se/Cu ratio for both the samples deposited at −0.4 V and −0.6 V along with the elemental atomic percentage concentration is tabulated in Table 2. It was observed that the agitation rate plays an important role to control the elemental concentration in the deposit. The results obtained for the sample deposited at −0.6 V without agitation are close to the stoichiometry.

Fig. 7 (A) shows the plot of $(\alpha h\upsilon)^2$ versus $(h\upsilon)$ of the layer deposited at −0.4 V for different agitation speeds. The values of band gap for the CIS layer deposited without agitation and with agitation at 100 rpm were estimated ~1.3 eV and ~1.48 eV, respectively. Both values are higher than that of the literature value (~1.05 eV) due to the growth of off stoichiometrc CIS layer, which resulted the formation of secondary phases of Cu_xSe_y along with CIS. The films deposited at 200 rpm shows the band gap of 1.91 eV which corresponds to band gap of copper selenide. Fig. 7 (B) shows the plot of $(\alpha h\upsilon)^2$ verses $(h\upsilon)$ for the layer deposited at −0.6 V for different agitation speeds. The band gap for the sample deposited without agitation was found to be 1.13 eV and with agitation at 100 rpm and 200 rpm was estimated ~1.30 eV and ~1.54 eV, respectively. The increased band gap is associated to the presence of binary compounds copper selenide and/or variation in grain size. The band gap estimated for the sample deposited at −0.6 V without agitation is close to the reported values of CIS thin films [33].

4. Conclusions

In summary, we have studied the effect of agitation on the electrodepostion of CIS thin films and their properties. Two growth potentials −0.4 V and −0.6 V verses Ag/AgCl reference electrode were optimized by CV measurements. Chronoamperometric curves show diffusive controlled growth with instantaneous nucleation. The layers deposited without agitation for both potentials were revealed polycrystalline CIS with tetragonal chalcopyrite crystal structure. On the contrary with increasing the agitation speed the peaks related to CuSe are attributed alongwith the CIS reflection. Cu-rich films are electrodeposited for both potentials with agitation due to the decrease of diffusion layer thickness near the cathode, which is further supported to enhance the limiting current density. The results obtained from Raman spectra are in good agreement with XRD and EDAX results. The surface morphology of the layer was found to be highly dependent on deposition potentials and agitation speeds. The globular grains deposited at −0.6 V without agitation are suitable for the preparation of high efficiency CIS based solar cell devices. Nearly stoichiometric CIS layers are deposited at −0.6 V without agitation. By employing external agitation a remarkable variation in In/Cu ratio was observed which also confirmed the deposition of copper is diffusion limited process. The results obtained by EDAX agrees well with the straructural data obtained by XRD. The deviation in the estimated energy band gap is proposed due to the prsence of secondary phases of CuSe, the variation in particle size or inhomogeneous growth of CIS. The post-depostion heat treatment could further enhance the crystallinity, particle size and would be helpful to obtain the stoichiometric CIS layer with optimum band gap.

Acknowledgments

The authors would like to thank the Defense research and development organization (DRDO) (ERIP/ER/10003866/M/01/1388) and CSIR (CSIR fellowship No. 09/137/(558)/2015-EMR-I) for financial support under the senior research fellowship program. Authors are thankful to UPE phase (II), under this program the Raman spectroscopy was used.

References

[1] M.A. Green, K. Emery, Y. Hishikawa, W. Warta, E.D. Dunlop, Solar cell efficiency tables (version 45), Prog. Photovolt. Res. Appl. 23 (2015) 1–9.
[2] http://www.pv-magazine.com/news/details/beitrag/zsw-sets-217-thin-film-efficiency-record_100016505/#axzz3q32i8kDu.
[3] A.H. Moharram, M.M. Hafiz, A. Salem, Electrical properties and structural changes of thermally co-evaporated $CuInSe_2$ films, Appl. Surf. Sci. 172 (2001) 61–67.
[5] I. Repins, M. Contreras, B. Egaas, D. Clay, J. Scharf, C. Perkins, B. To, R. Noufi, 19.9% efficient ZnO/CdS/$CuInGaSe_2$ solar cell with 81.2% fill factor, Prog. Photovolt. Res. Appl. 16 (2008) 235–239.
[6] T. Terasako, Y. Uno, T. Kariya, Structural and optical properties In-rich $CuInSe_2$ polycrystalline thin films prepared by chemical spray pyrolysis, Sol. Energy Mater. Sol. Cells 90 (2006) 262–275.
[7] S. Niki, A. Yamada, R. Hunger, Molecular beam epitaxial growth and characterization of CuInSe2 and CuGaSe2 for device applications, J. Cryst. Growth 237–239 (2002) 1993–1999.
[8] A.N. Tiwari, M. Krejci, F.J. Haug, H. Zogg, 12.8% efficiency Cu(In,Ga)Se_2 solar cell on a flexible polymer sheet, Prog. Photovolt. Res. Appl. 7 (1999) 393–397.
[9] A. Ashida, Y. Hachiuma, N. Yamamoyo, Y. Cho, $CuInSe_2$ thin films prepared by quasi-flash evaporation of In_2Se_3 and Cu_2Se, J. Mater. Sci. Lett. 13 (1994) 1181–1184.
[10] X.L. Wang, G.J. Wang, B.L. Tian, Z.L. Du, $CuInSe_2$ thin films obtained by pulse-plating electrodeposition technique with novel pulse wave, Chin. Sci. Bull. 55 (2010) 1854–1858.
[11] H. Lee, W. Lee, J. Kim, M. Ko, K. Kim, K. Seo, D. Lee, H. Kim, Highly dense and crystalline $CuInSe_2$ thin films prepared by single bath electrochemical deposition, Electrochim. Acta 12 (2013) 450–456.

[13] N.B. Chaure, J. Young, A.P. Samantilleke, I.M. Dharmadasa, Electrodeposition of n-i-p-type $CuInSe_2$ multilayers for photovoltaic application, Sol. Energy Mater. Sol. Cells 81 (2004) 125–133.
[14] P.U. Londhe, A.B. Rohom, N.B. Chaure, $CuInSe_2$ thin film solar cells prepared by low-cost electrodeposition techniques from a non-aqueous bath, RSC Adv. 5 (2015) 89635–89643.
[15] R.N. Bhattachrya, J.F. Hiltner, W. Batchelar, M.A. Contreras, R.N. Noufi, J.R. Sites, 15.4% $CuIn_{1-x}GaxSe_2$-based photovoltaic cells from solution-based precursor films, Thin Solid Films 361–362 (2000) 396–399.
[16] N.B. Chaure, A.P. Samantilleke, I.M. Dharmadasa, The effects of inclusion of iodine in CdTe thin films on material properties and solar cell performance, Sol. Energy Mater. Sol. Cells 77 (2003) 303–317.
[17] M. Maldes, M. Vazquez, A. Goossens, Electrodeposition of $CuInSe_2$ and In_2Se_3 on flat and nanoporous TiO_2 substrates, Electrochim. Acta 54 (2008) 524–529.
[18] A.B. Rohom, P.U. Londhe, N.B. Chaure, The effect of pH and selenization on the properties of $CuInSe_2$ thin films prepared by electrodeposition technique for device Applications, J. Solid State Electrochem. 19 (2015) 201–210.
[19] P.U. Londhe, A.B. Rohom, N.B. Chaure, Selenization of electrodeposited copper–indium alloy thin films for solar cell applications, J. Mater. Sci. Mater. Electron. 25 (2014) 4643–4649.
[20] A. Burgos, R.S. Schrebler, H. Gomez, F.A. Cantano, R.E. Marotti, E.A. Dalchiele, Potential pulsed electrodeposition of $CuInSe_2$ thin films, Int. J. Electrochem. Sci. 10 (2015) 10543–10553.
[21] S. Nakamura, S. Sugawara, A. Hashimoto, A. Yamamoto, Composition control of electrodeposited Cu-In-Se layers for thin film $CuInSe_2$ preparation, Sol. Energy Mater. Sol. Cells 50 (1998) 25–30.
[22] F. Lai, F. Liu, Z. Zhang, J. Liu, Y. Li, S. Kung, J. Li, Y. Liu, Cyclic voltammetry study of electrodeposition of $Cu(In,Ga)Se_2$ thin films, Electrochim. Acta 54 (2009) 3004–3010.
[23] A.J. Bard, L.R. Faulkner, John Wiley and Sons Inc., New York, second ed., 2001.
[24] W. Chen, Y. He, W. Gao, Synthesis of nanostructured Ni-TiO2 composite coatings by Sol-enhanced electroplating, J. Electrochem. Soc. 157 (2010), E122.
[25] N. Kanuri, Electroplating, Basic Principles, Processes and Practices, Elsevier advanced Technology, Oxford, 2004.
[26] Y.D. Gamburg, G. Zangari, Theory and Practice of Metal Electrodeposition, Springer, 2011.
[27] S.S. Djokic, Electrodeposition; Theory and Practices, Springer, 37, Sol. Energy Mater. Sol. Cells 109 (2013) 17–25.
[28] A. Cho, S. Ahn, J.H. Yun, J.G. Wak, S.K. Ahn, K. Shin, H. Song, K.H. Yoon, Non-vacuum processed $CuInSe_2$ thin films fabricated with a hybrid ink, Sol. Energy Mater. Sol. Cells 109 (2013) 17.
[29] W. Witte, R. Kniese, M. Powalla, Raman investigation of $Cu(In,Ga)Se_2$ thin films with various copper contents, Thin Solid Films 517 (2008) 867–869.
[30] E. Chassaing, O. Ramdani, P.P. Grand, J.F. Guillemoles, D. Lincot, New insights in the electrodeposition mechanism of $CuInSe^2$ thin films for solar cell application, Phys. Status Solidi C 5 (2008) 3445.
[31] L. Thouin, S. Massaccesi, S. Sanchez, J. Vedal, Formation of copper indium diselenide by electrodeposition, J. Electroanal. Chem. 374 (1994) 81–88.
[32] N.D. Nikolić, K.I. Popov, L.J. Pavlović, M.G. Pavlović, The effect of hydrogen codeposition on the morphology of copper electrodeposits. I. The concept of effective overpotential, J. Electroanal. Chem. 588 (2006) 88–98.
[33] O.P. Agnihotri, P. Raja Ram, R. Thangaraj, A.K. Sharma, A. Raturi, Structural and optical properties of sprayed $CuInSe_2$ films, Thin Solid Films 102 (1983) 291–297.